University of Califorina at Davis, Center for Geotechnical Modeling Report UCD-CGM-01
Published in the Communications in Numerical Methods in Engineering, Vol. 15, pages 867-876, 1999.

Application of the p–version of the Finite Element Method to Elasto–plasticity with Localization of Deformation

Boris Jeremić [1] **Christos Xenophontos** [2]

Abstract

In this paper we discuss the use of the p–version of the finite element method applied to elasto–plastic problems that exhibit sharp (but continuous) deformation gradients. The deformation theory of deviatoric, linearly hardening elasto–plasticity with an iterative, displacement based finite element framework is used. The focus of this work is on assessing the applicability of the p–version to the analysis of localized deformation with continuous strain and displacement fields. Presented examples demonstrate that the method can be used reliably with a proper finite element mesh design. Possible extensions of the work are also discussed.

[1] Department of Civil and Environmental Engineering, University of California, Davis, CA, 95616, phone (530) 2754-9248, fax (530) 756-7872 email: `jeremic@ucdavis.edu`

[2] Department of Mathematics and Computer Science, Clarkson University, Potsdam, NY 13699, phone (315) 268-2387, fax (315) 268-6670 email: `christos@clarkson.edu`

Key Words: finite element method, p–version, elasto–plasticity, localization of deformation

1 Introduction

A phenomenon that accompanies elasto–plastic deformation of solids is the formation of localized bands of considerable straining. The phenomenon of localization can be observed in a wide variety of engineering solids such as metals, sands, clays and soft rocks. One possible approach to capture the localization is to enhance the low order finite elements with suitably defined shape functions which mimic localized deformation [8]. Another possibility is to use discontinuous shape functions to enhance the non–smooth plastic solution [5], [1]. Current work on finite element solid modeling of the localization of deformation is mostly focused on the discontinuous bifurcation of the strain–rate field [10], [9], [1], [8]. There exist, however, cases where the localization is characterized by sharp, but *continuous* deformation gradients. Such cases include, but are not limited to, the modeling of ductile geomaterials (sands, clays, etc), which is a major motivation for this work. Large shear deformations in sand, for example, tend to be localized in narrow bands with approximately 3-20 grain diameters in size [14], [7]. Deformation is continuous, with sharp gradients across the localized material.

The standard Finite Element Method (FEM), and in particular the p–version of the FEM that includes a rather rich displacement field, can be used reliably for these types of problems. Unlike the traditional h–version, the p–version uses piecewise polynomials of *varying* degree over a *fixed* mesh to approximate the solution to a boundary value problem. One main advantage of the p–version is that for linear problems whose solution is analytic, the rate of convergence is *exponential*. This is true even if the solution is analytic with the exception of a finite number of (singular) points, provided the mesh is designed accordingly. Thus, by examining the given data (loads, boundary conditions and shape of the domain) one can design the mesh and degree distribution for the p–

version accordingly, and achieve exponential rates of convergence. For certain types of non-linear problems, e.g., problems with material non-linearities arising in non-linear elasticity and elasto–plasticity, the smoothness of the solution is not significantly perturbed. Hence, the p–version can be effectively applied, as can be seen by the results of Szabó et al. [12] and Holzer and Yosibash [3]. We should mention that in [12] the deformation theory of plasticity is used while the results in [3] rely on the incremental theory of plasticity.

The purpose of this paper is to assess the applicability of the p–version to elasto–plastic problems exhibiting localization of deformation. We follow the approach described in [12], in which the deformation theory of plasticity is used in conjunction with an iterative scheme to solve the non-linear problem. We consider two model problems arising from engineering applications, whose solution exhibits such localization effects. The paper is organized as follows: in Section 2 we briefly review the deformation theory of plasticity and the specific numerical algorithm used for this study. The model problems are described in Section 3 and our numerical results appear in Section 4.

2 Deformation Theory of Plasticity

The deformation theory of plasticity assumes that stresses determine strains uniquely as long as the plastic deformation continues. The additive decomposition of the total strain field is written as

$$\epsilon_{ij}^{p} = \epsilon_{ij} - \epsilon_{ij}^{e} = f_{ij}(\sigma_{kl}) \ , \tag{1}$$

where ϵ_{ij}^{p} is the plastic component of the strain tensor, ϵ_{ij}^{e} is the elastic component and ϵ_{ij} is the total strain tensor. The deformation theory of plasticity is valid only for the case of proportional or radial loading, in which ratios among the stress components remain constant. The basic assumptions (cf. [2], [6]) for the deformation theory of plasticity are the following: the material is isotropic, only deviatoric plastic strains occur, elastic strains obey generalized Hooke's law, principal axes of the plastic stress and strain coincide, ratios of principal values of the plastic strain have same values as ratios of principal values of stress deviator.

The generalized Hooke's law can be written as

$$\sigma_{ij} = E_{ijkl}\epsilon^{e}_{kl} \ , \tag{2}$$

where the elastic tangent stiffness tensor E_{ijkl} can be written in terms of Lamé's constants λ and μ as

$$E_{ijkl} = \lambda\delta_{ij}\delta_{kl} + \mu\left(\delta_{ik}\delta_{jl} + \delta_{il}\delta_{jk}\right) \ . \tag{3}$$

The plastic strain ϵ^{p}_{ij} has deviatoric components only, hence $\epsilon^{p}_{kk} = 0$. The deviatoric plastic strains can be related to the deviatoric stress ${}^{dev}\sigma_{ij}$ as

$${}^{dev}\epsilon^{p}_{ij} = \Phi \ {}^{dev}\sigma_{ij} \quad , \quad {}^{dev}\sigma_{ij} = \sigma_{ij} - \frac{1}{3}\sigma_{kk}\delta_{ij} \ . \tag{4}$$

The function Φ, which controls the response, can be calibrated from experimental stress strain curves by using effective stresses $\bar{\sigma}$ and effective plastic strains $\bar{\epsilon}^{p}$, defined as

$$\bar{\sigma} = \sqrt{\frac{3}{2} \, {}^{dev}\sigma_{ij} \, {}^{dev}\sigma_{ij}} \ , \tag{5}$$

$$\bar{\epsilon}^{p} = \sqrt{\frac{2}{3} \, {}^{dev}\epsilon^{p}_{ij} \, {}^{dev}\epsilon^{p}_{ij}} \ . \tag{6}$$

One of the simplest effective stress – effective strain curves follows a bilinear law. For the elastic ($\bar{\epsilon} \leq \epsilon_{yield}$) and plastic ($\bar{\epsilon} > \epsilon_{yield}$) region we can write the secant relation

$$\bar{\sigma} = \begin{cases} E \ \bar{\epsilon}^{e} & \bar{\epsilon} \leq \epsilon_{yield} \\ E_s \ \bar{\epsilon} & \bar{\epsilon} > \epsilon_{yield} \end{cases} \ , \tag{7}$$

where E_s is the secant modulus (see Figure 1).

[FIGURE 1 ABOUT HERE]

The p–version of the FEM can be applied to elasto–plastic problems based on the deformation theory of plasticity, in the following sequence of steps.

- Obtain a solution for the linear elastic problem. Perform p extension from $p = 1$ (linear elements) to, say $p = 8$. Note the p level for which the (estimated) relative error in the energy norm is less than 5 % (preferably less than 1%).

- Using the solution obtained for the accepted p level perform an iterative analysis for the elasto–plastic computations. The actual algorithm, called *direct iteration*, is described in more detail below (cf. [12]).

  1. Compute $\bar{\epsilon}$ in each Gauss point (from the elastic solution) and set the first iterative effective strain $\bar{\epsilon}^{[1]} := \bar{\epsilon}^{e}$.
  2. Using $\bar{\epsilon}^{[k]}$, compute the secant modulus $E_s^{[k]}$ for each Gauss point from the effective stress – effective strain curve (Figure 1).
  3. In each Gauss point for which $\bar{\epsilon}^{[k]} > \bar{\epsilon}_{yield}$, determine the elastic-plastic material stiffness matrix. Obtain a new finite element solution $u_{FE}^{[k+1]}$.
  4. Using $E_s^{[k]}$ and $u_{FE}^{[k+1]}$, compute the stress tensor components $\sigma_{ij}^{[k+1]}$ in each Gauss point, using the total strain computed from $u_{FE}^{[k+1]}$ and the elastic-plastic material stiffness matrix. Determine the elastic strains from $\sigma_{ij}^{[k+1]}$, the elastic part of the material stiffness matrix, and compute the plastic strain from (1).
  5. Calculate the effective elastic strain $\bar{\epsilon}^{e\ [k+1]}$, effective plastic strain $\bar{\epsilon}^{p\ [k+1]}$, and total effective strain $\bar{\epsilon}^{[k+1]}$. The iterations stop when at each Gauss point

     $$\frac{\left|\bar{\epsilon}^{[k+1]} - \bar{\epsilon}^{[k]}\right|}{\bar{\epsilon}^{[k+1]}} \leq tol \qquad (8)$$

     where *tol* is a user prescribed tolerance. If, on the other hand, the tolerance criterion is not met, using $\bar{\epsilon}^{[k+1]}$ compute $E_s^{[k]}$, increment k to $k+1$ and return to step 2.

It is important to note that in this algorithm there are no load increments, but load is rather applied in one step. This simplification is possible for proportional loading paths, which is the case in the examples we will be examining. A more general approach would be to use the incremental, flow theory of plasticity, which will enable computations with general load paths. For the purpose of this study we use a simple elastic–plastic deviatoric model with linear isotropic hardening in effective stress – effective strain space. The numerical examples presented in Section 4 were based on the direct iteration algorithm described above.

It should be noted that large strains occur in continuous shear bands. Theoretically sound approach would be to use large deformation postulates. We are indeed working on incorporating recently developed large deformation theory for geomaterials ([4]) in our p–version FEM code.

3 The model problems

3.1 Rigid indentation of a plane strain solid

We consider a square plane strain solid of unit area with the bilinear material characteristics $E = 3 \times 10^7$ kN/m^2, $\nu = 0.3, E_t = 2 \times 10^4$ kN/m^2, $\sigma_{yield} = 3 \times 10^4$ kN/m^2, and boundary conditions as shown in Figure 2(a). For the computations in Section 4, $\Delta = 1 \times 10^{-2}$, except for the results shown in Figure 6. This kind of deviatoric plasticity problems is usually found in failure mechanics of metals and locally undrained soils (clays), among others.

[FIGURE 2 ABOUT HERE]

We expect (c.f. [11]) a shear band to form at a -45^o angle, emanating from the point (1/3, 1). Schreyer and Neilsen [11] used an elastic–plastic softening material in order to enhance the shear band formation. With a softening branch in equivalent stress – equivalent strain space, the localized zone is narrower since the material outside the localized zone is elastically unloading. In this study, we use an elastic–plastic hardening material which yields a narrow shear zone exactly positioned as expected.

The design of the mesh for this model problem is shown in Figure 2(b). Since we expect the (linear) solution to have a singularity at the point where the displacement load is imposed, we use a non-uniform but fixed mesh with 25 elements. The effect of having more elements near the point of singularity can be seen (and justified) through the numerical results in the next section.

3.2 Slope stability problem

Next, we consider a slope stability problem, as seen in Figure 3(a).

[FIGURE 3 ABOUT HERE]

In this case a steep slope in overconsolidated clay is loaded in displacement control by a rigid indentation. We expect a localized zone of shear deformation to propagate from the end of the rigid vertical indentation load toward the slope surface. The bilinear material characteristics used for this model are $E = 3 \times 10^4$ kN/m^2, $\nu = 0.3, E_t = 2 \times 10^1$ kN/m^2, $\sigma_{yield} = 1 \times 10^2$ kN/m^2, and the boundary conditions are as shown in Figure 3(a). It is important to note that the material is saturated clay with low permeability, which for a relatively fast loading, can be treated as totally undrained thus allowing the use of deviatoric elasto–plastic material analysis.

As in the previous model, we again use a non-uniform mesh (with 24 elements) to capture the singularity present in the solution (see Figure 3(b)).

4 Numerical Results

In this section we present the results of numerical computations for the problems described in Section 3. The product polynomial space was used, with p varying uniformly from 1 to 8 over all elements in the fixed mesh.

For both problems the estimated relative error for the linear solution, measured in the energy norm, was less than 2.5% for $p = 8$. Using the solution of the linear problem (with $p = 8$) as our initial FEM solution, we performed the nonlinear iterations with allowable tolerance 1%. Figure 4 shows the contour plot of the equivalent strain $\bar{\epsilon}$ for the first problem. As expected, see e.g. [11], a localized zone of deformation propagates from the singular point to the side.

[FIGURE 4 ABOUT HERE]

It is also worth showing (see Figure 5) how the increase in the polynomial degree, affects the final result. Note that as p increases, the results quickly become more accurate and the localization zone becomes more pronounced. In particular, once $p \geq 5$ the shear band is captured extremely well and the result does not change significantly.

[FIGURE 5 ABOUT HERE]

Moreover, the progression of the plastic, localized zone as the applied displacement

Δ changes is shown Figure 6. It should be mentioned that this progression analysis was performed in a number of purely iterative steps.

[FIGURE 6 ABOUT HERE]

The issue of proper mesh design is illustrated by an example. In Figure 7 we show a 3 by 3 and a 12 by 12 uniform mesh for the same model problem. The first mesh lacks refinement and the localized shear zone is artificially curved. The second mesh is finer but is still not properly designed and the shear zone does not propagate as expected. We should mention that this phenomenon can be eliminated through the use of a *sufficiently* fine uniform mesh. This, however, would require the degrees of freedom to go beyond "practical" limits. The non-uniform mesh proposed here allows us to correctly predict the shear band without using a large number of elements.

[FIGURE 7 ABOUT HERE]

We now turn our attention to the second model problem, which was solved following the same sequence of analysis steps as the previous one. Figure 8 shows the localized shear zone developed from the rigid indentation on the soil slope, for $p = 8$ and $\Delta = 0.075$. A roughly circular zone of intense shearing develops starting from the singular point (end of rigid punch) and propagates toward the slope, as expected [13]. Similar results were obtained by Armero and Garikipati [1]. It should be mentioned that in our case the shear zone is continuous, unlike in the solutions obtained by Armero and Garikipati [1] who used discontinuous shape functions enrichment in their analysis.

[FIGURE 8 ABOUT HERE]

5 Conclusions

In this paper we have investigated use of the p–version of the FEM in elasto–plasticity and in particular the modeling of continuous, sharp displacement gradients in solid mechanics. Our numerical experiments show that even the simple deformation theory of plasticity gives very good results. Moreover, we note that the use of the p–version of the FEM in conjunction with non-uniform but fixed meshes enabled us to accurately predict the shear band formation, *without* the use of enhanced finite element spaces and/or special basis functions. The method is very efficient computationally and it is available in standard FEM commercial codes, based on the deformation theory of plasticity.

These observations suggest that it would beneficial to extend the use of the p–version of the FEM to the incremental, large deformation elasto–plastic theories. The application to problems in failure mechanics of engineering solids would be of great interest. Results in this direction will be presented in forthcoming papers.

References

[1] Armero, F., and Garikipati, K. An analysis of strong discontinuity in multiplicative finite strain plasticity and their relation with the numerical simulation of strain localization in solids. *International Journal of Solids and Structures 33*, 20-22 (1996), 2863–2885.

[2] Chen, W. F., and Han, D. J. *Plasticity for Structural Engineers.* Springer Verlag, 1988.

[3] Holzer, S. M., and Yosibash, Z. The p–version of the finite element method in incremental elasto–plastic analysis. *International Journal for Numerical Method in Engineering 39* (1996), 1859–1878.

[4] Jeremić, B., Runesson, K., and Sture, S. A model for elastic–plastic pressure sensitive materials subjected to large deformations. *International Journal of Solids and Structures 36*, 31/32 (1999), 4901–4918.

[5] Johnson, C., and Scott, R. A finite element method for problems in perfect plasticity using discontinuous trial functions. In *Nonlinear Finite Element Analysis in Structural Mechanics* (1981), W. Wunderlich, E. Stein, and K.-J. Bathe, Eds., Springer Berlin, pp. 307–324.

[6] Lubliner, J. *Plasticity Theory.* Macmillan Publishing Company, New York., 1990.

[7] Nemat-Nasser, S., and Okada, N. Strain localization in particulate media. In *Proceedings of the 12th Engineering Mechanics Conference* (May 17-20 1998), H. Murakami and J. E. Luco, Eds., ASCE.

[8] Ortiz, M., Leroy, Y., and Needleman, A. A finite element method for localized failure analysis. *Computer Methods in Applied Mechanics and Engineering 61* (1987), 189–214.

[9] Ottosen, N. S., and Runesson, K. Properties of discontinuous bifurcation solutions in elasto–plasticity. *International Journal of Solids and Structures 27*, 4 (1991), 401–421.

[10] Rudnicki, J. W., and Rice, J. R. Conditions for the localization of deformation in pressure–sensitive dilatant materials. *Journal of the Mechanics and Physics of Solids 23* (1975), 371 to 394.

[11] Schreyer, H. L., and Nielsen, M. K. Analytical and numerical tests for loss of material stability. *International Journal for Numerical Methods in Engineering 39* (1996), 1721–1736.

[12] Szabó, B. A., Actis, R. L., and Holzer, S. M. Solution of elastic–plastic stress analysis problems by the p–version of the finite element method. In *The IMA Volumes in Mathematics and its Application*, J. E. F. e. a. I. Babuška, Ed., vol. 75. Institute of Mathematics and its Applications, University of Minnesota, Springer, New York, 1993, pp. 395–416.

[13] Terzaghi, K., Peck, R. B., and Mesri, G. *Soil Mechanics in Engineering Practice*, third ed. John Wiley & Sons, Inc., 1996.

[14] Vardoulakis, I., and Sulem, J. *Bifurcation Analysis in Geomechanics*. Blackie Academic & Professional, 1995. ISBN 0-7514-0214-1.

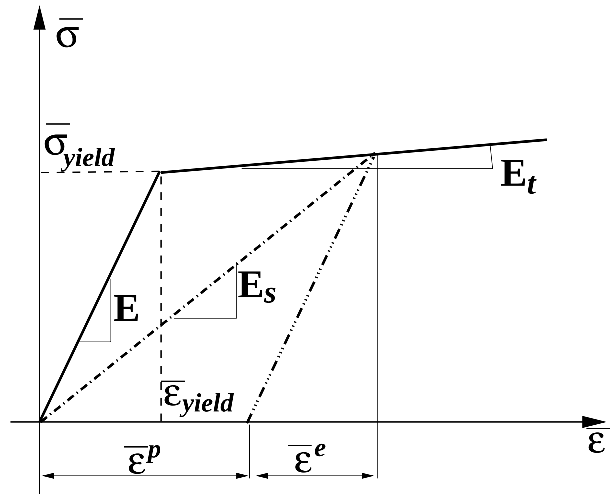

Figure 1: Elastic plastic effective stress effective strain bilinear model

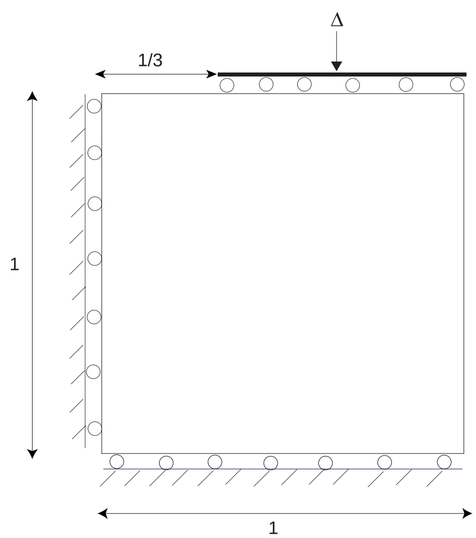

a)

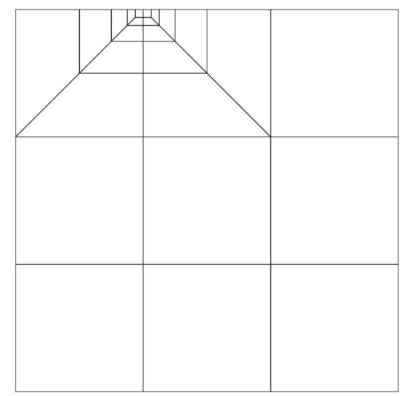

b)

Figure 2: (a) Geometry of model with load and boundary conditions. (b) The non-uniform mesh for model 1.

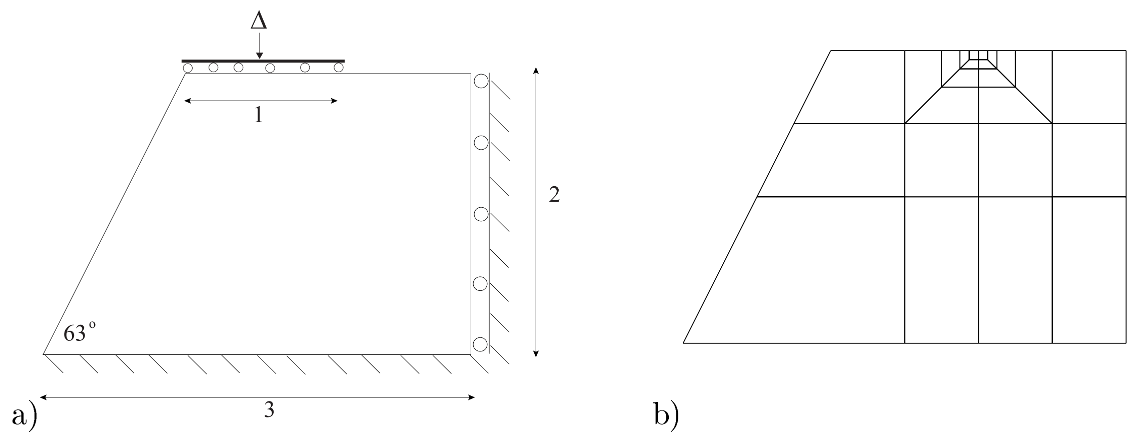

Figure 3: (a) Geometry of model with load and boundary conditions. (b) The non-uniform mesh for model 2.

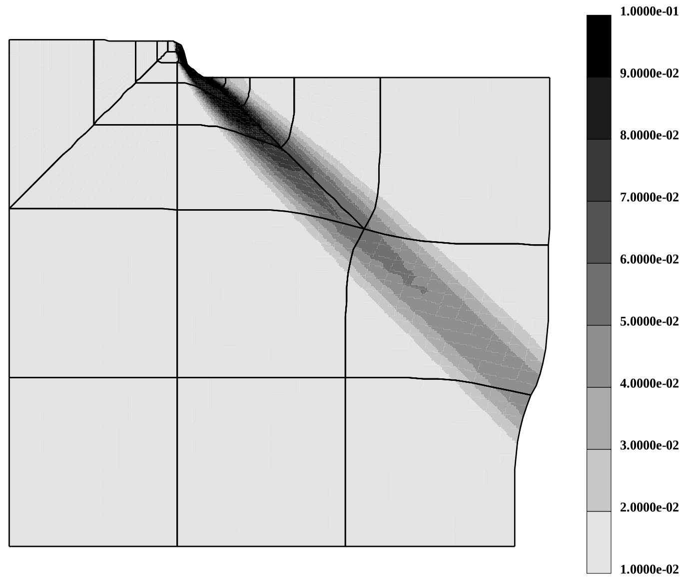

Figure 4: Equivalent strain $\bar{\epsilon}$ for $p = 8$.

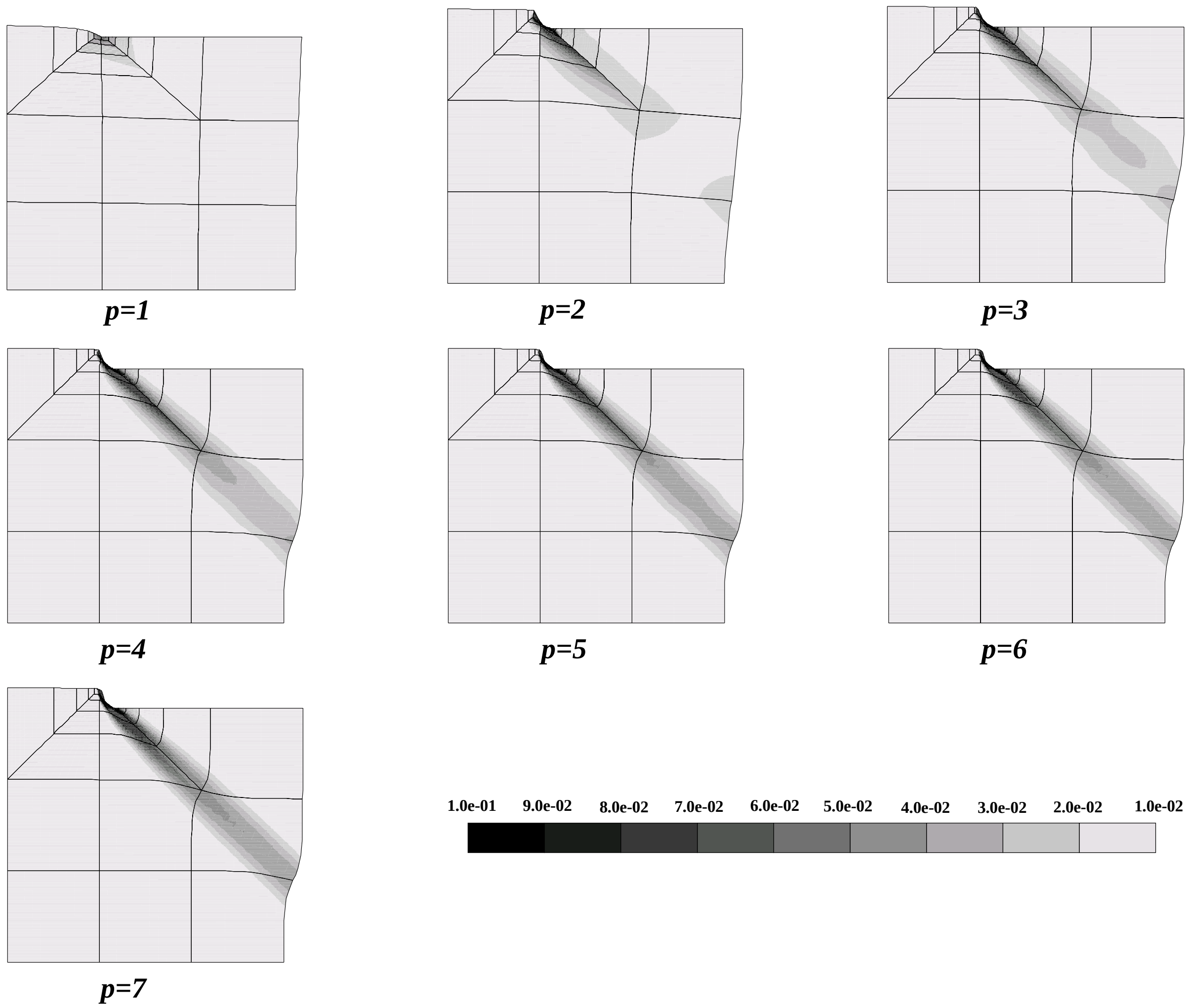

Figure 5: Equivalent strain $\bar{\epsilon}$.

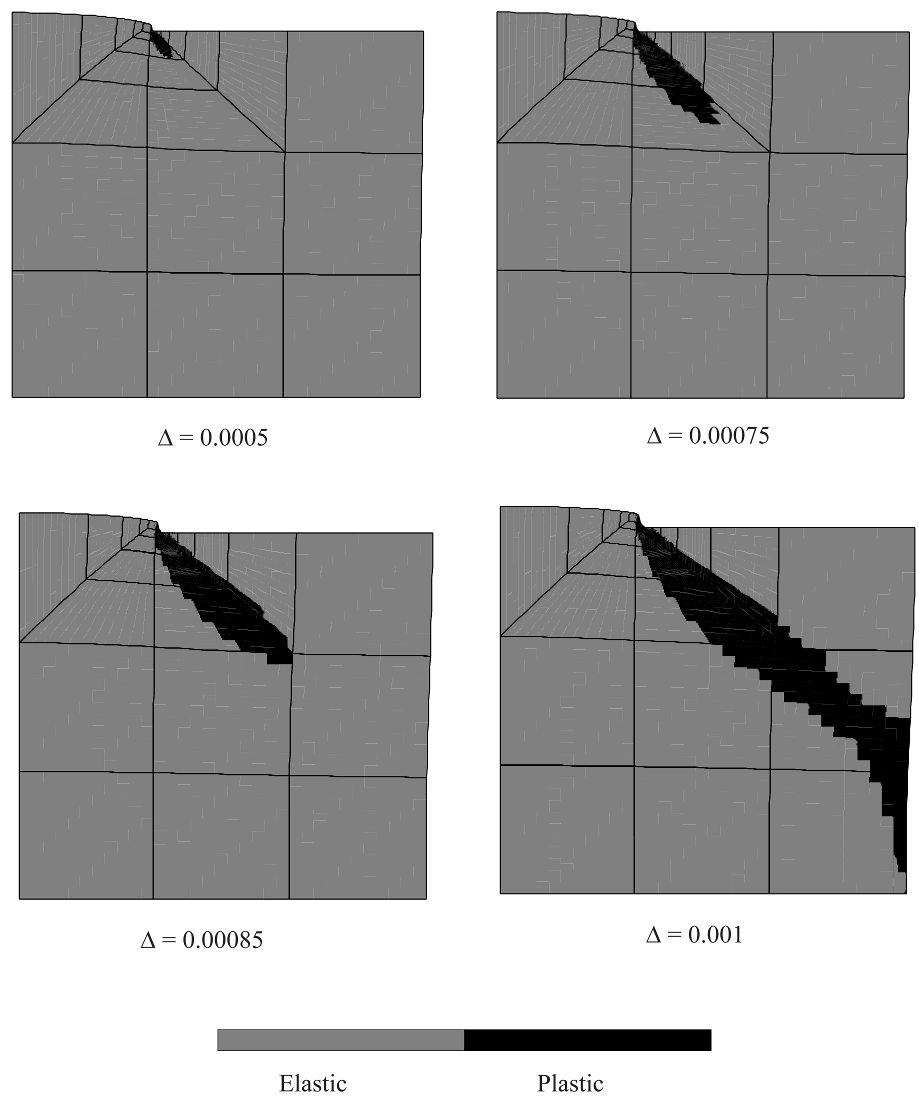

Figure 6: Progression of the localized plastic zone for $p = 8$.

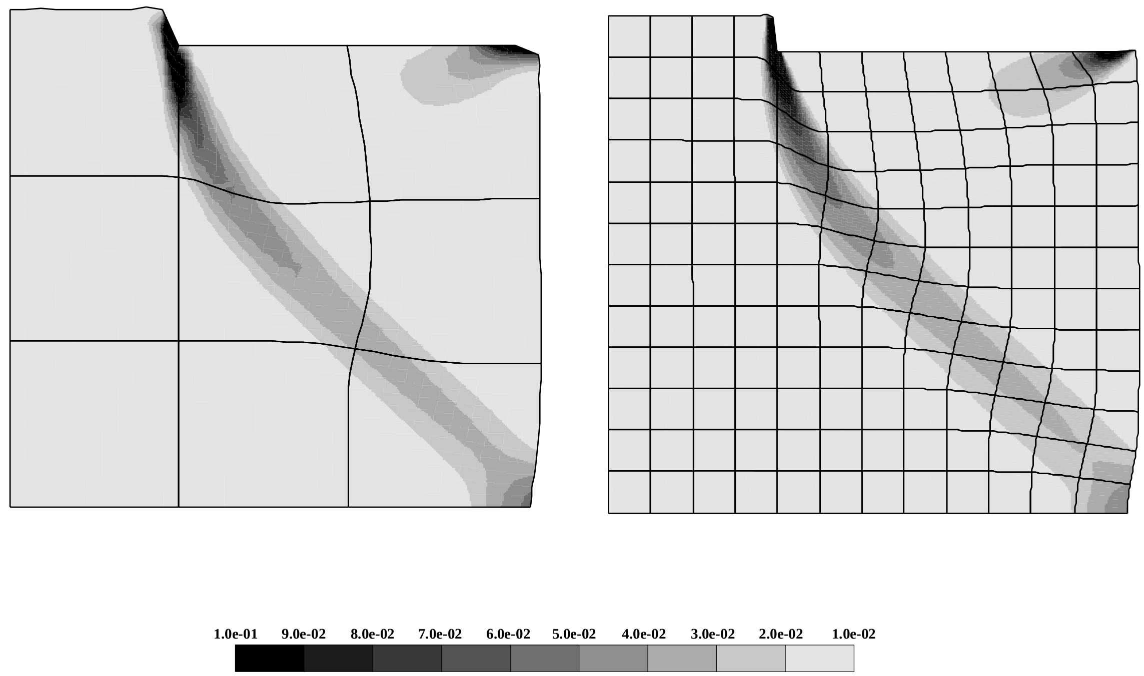

Figure 7: Equivalent strain $\bar{\epsilon}$ for 3 by 3 mesh and 12 by 12 mesh, $p = 8$.

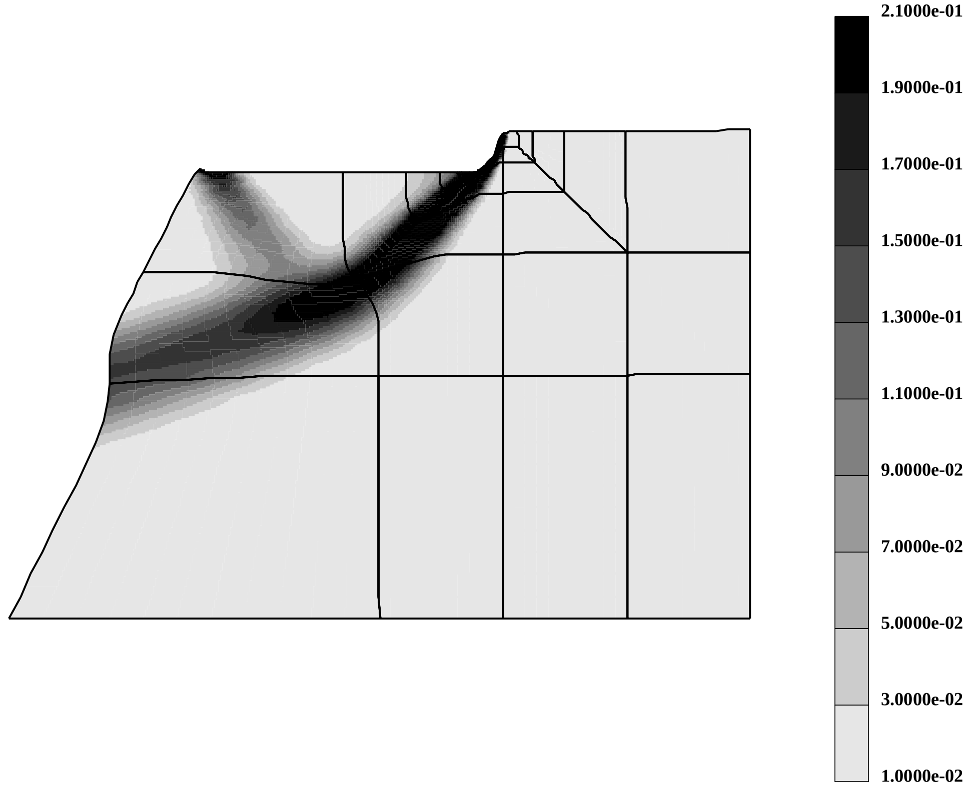

Figure 8: Equivalent strain $\bar{\epsilon}$ for the slope stability problem, $p = 8$.